Proc. Natl. Acad. Sci. USA
Vol. 96, pp. 10881–10886, September 1999
Microbiology

Cytomegalovirus-encoded β chemokine promotes monocyte-associated viremia in the host

NOAH SAEDERUP*, YU CHUN LIN*†, DANIEL J. DAIRAGHI‡, THOMAS J. SCHALL‡, AND EDWARD S. MOCARSKI*§

*Department of Microbiology and Immunology, Stanford University Medical School, Stanford, CA 94305-5124; and ‡ChemoCentryx, 1539 Industrial Road, San Carlos, CA 94070

Communicated by Mark M. Davis, Stanford University School of Medicine, Stanford, CA, July 12, 1999 (received for review April 24, 1999)

ABSTRACT **Chemokine homologs are encoded by many large DNA viruses, suggesting that they contribute to control of host leukocyte transmigration and trafficking during viral infection. Murine cytomegalovirus carries a CC (β) chemokine homolog gene giving rise to two related proteins, murine cytomegalovirus chemokine 1 and 2 (MCK-1 and MCK-2). MCK-1 peptide was found to induce calcium signaling and adherence in murine peritoneal macrophages. Cells bearing human chemokine receptor CCR3 and the human macrophage THP1 cell line were responsive to MCK-1. This pattern suggested that MCK-1 might act as an agonist, promoting leukocyte trafficking during viral infection. Consistent with this prediction, MCK-1/MCK-2 mutant viruses exhibit dramatically reduced peak levels of monocyte-associated viremia in experimentally infected mice. Thus, MCK-1/MCK-2 appears to promote host leukocyte migration to initial sites of infection and may be responsible for attracting monocytes or macrophages that efficiently disseminate virus in the host.**

The genomes of herpesviruses and poxviruses contain cellular homologs of small, chemoattractant cytokines, called chemokines (1, 2), although their function during virus infection is not yet clear (3–10). Chemokines normally serve to coordinate trafficking of peripheral blood (PB) leukocytes by stimulating adhesion, chemotaxis, transmigration, and other immune effector functions through chemokine receptors (2). Virus-encoded β (CC) chemokine homologs encoded by the molluscum contagiosum poxvirus MC148 gene and the Kaposi's sarcoma herpesvirus vMIP-II gene have been shown to either activate or antagonize chemokine receptors (4, 5, 8–10). Human cytomegalovirus (CMV) has recently been shown to encode a potent α (CXC) chemokine capable of attracting neutrophils (6). In addition to possible roles in modulating local inflammatory responses or development of an adaptive antiviral immune response, virus-encoded chemokines may directly influence leukocyte trafficking and favor efficient dissemination via motile immune cell populations. Many viral infections, including those of human (11) and murine CMV (12–14), proceed through a leukocyte-associated viremia, which likely plays a significant role in viral dissemination.

Although a significant amount of information has been generated to understand basic structure, replication, and pathogenesis of human CMV (15), further insights into interactions with the host need to be modeled through study of such viruses as murine CMV, a natural mouse pathogen (16). The murine CMV genome contains >160 nonoverlapping ORFs organized in a manner that is collinear to human CMV (17). The carboxyl terminus of one ORF, designated m131, has been predicted to encode an 81-aa product from an 850- to 900-nt (γ0.85) true late transcript expressed during productive infection (3, 12, 18). This predicted gene product was designated murine CMV chemokine 1 (MCK-1) because of sequence similarity to host β chemokines (ref. 3; Fig. 1*A*). Despite having only limited homology to mammalian chemokines (see Fig. 1*A*), and even less relatedness to the CXC chemokine homologs found in human CMV (6), MCK-1 has retained hallmark chemokine sequence characteristics, including a predicted amino-terminal signal peptide and canonical β chemokine cysteine spacing (2, 3). Recently, a second gene product, denoted MCK-2, was characterized as a fusion between MCK-1 and a downstream ORF, m129 (7). Both MCK-1 and MCK-2 have the same chemokine domain encoded by a portion of m131. MCK-2 contains an additional 199-aa novel carboxyl terminus as a result of RNA splicing.

Murine CMV disseminates via mononuclear leukocytes (12, 13), most likely monocyte/macrophages, in two distinct phases during acute infection (14). A primary viremia peaks within 2 days after inoculation and initiates seeding of peripheral organs, including spleen and liver, but not salivary glands, a prominent site of viral replication that is responsible for transmission to new hosts. Seeding of the salivary gland, a poorly vascularized organ, depends on a secondary, more intense, viremia that peaks at 5–6 days postinoculation. These phases differ markedly in that the secondary viremia is associated with infection of PB monocyte/macrophages (12–14).

We have investigated the chemokine-like activities of MCK-1 and the role of the MCK-1/MCK-2 locus in control of viremia and dissemination in the natural host for murine CMV. Based on our observations, we propose that this viral function may be involved in recruiting and/or activating leukocyte subsets that act as vehicles for dissemination during acute infection.

MATERIALS AND METHODS

Chemokine Reagents, Cells, and Virus. RANTES, macrophage chemotactic protein 3 (MCP-3), murine and human eotaxin, and macrophage inflammatory protein 1α (MIP1α) were expressed in *Escherichia coli* and were purified by R & D Systems. MCK-1 was synthesized by Gryphon Sciences (South San Francisco, CA) starting at a threonine 19 amino acids downstream of the fourth methionine in the m131 ORF (3). Human CCR1, CCR2b, and CCR5 expressing NIH 3T3 cells were a gift of Dan Littman (New York University) and were constructed as described in ref. 19. Human and murine CCR3 cell lines were made in rat Y3 Ag1.2.3 cells (American Type Culture Collection CRL-1631) as described (20). Human CMV US28 cell lines were constructed in human 293 cells

The publication costs of this article were defrayed in part by page charge payment. This article must therefore be hereby marked "*advertisement*" in accordance with 18 U.S.C. §1734 solely to indicate this fact.

PNAS is available online at www.pnas.org.

Abbreviations: PB, peripheral blood; PBL, peripheral blood leukocyte; CMV, cytomegalovirus; MCK-1, murine CMV chemokine 1; MCP-3, macrophage chemotactic protein 3; MIP1α, macrophage inflammatory protein 1α; X-Gal, bromo-4-chloro-3-indolyl-β-D-galactopyranoside; PEC, peritoneal exudate cells.

†Present address: Institute of Preventative Medicine, National Defense Medical Center, P.O. Box 90048-700 Shanhsia, Taipei, Taiwan, Republic of China.

§To whom reprint requests should be addressed. E-mail: mocarski@stanford.edu.

(American Type Culture Collection CRL-1573) as described (21). Stocks of wild-type murine CMV strain K181$^+$ (12) and virus recombinants were grown and titered on NIH 3T3 cells (American Type Culture Collection CRL1658) as described (22). Supernatant harvested between 24 and 48 h after cultures reached 100% cytopathic effect was clarified of cell debris by centrifugation at 2,500 $\times$ *g*. Virus was collected by sedimentation at 17,000 $\times$ *g*, was suspended in cell growth medium, and was stored frozen in aliquots at -80°C until use. The titer of all stocks was confirmed at the time mice were inoculated.

Recombinant Viruses. RM427$^+$ and RM4485 were constructed by sequential transfection of NIH 3T3 cells with either *Bam*HI-linearized pON427 (22) or *Eco*RI-linearized pON4485 followed by infection with K181$^+$ at a multiplicity of infection of 3 as described by Vieira *et al.* (18). pON4485 contains a 6.6-kilobase *Dra*I/*Eco*RI DNA fragment spanning the *ie*1/*ie*2/*ie*3 enhancer, *ie*2 gene, γ0.85 transcript, and *sgg*1 gene inserted into pGEM-2 (Promega) where two modifications have been made: (*i*) a 79-bp *Hpa*I fragment in the promoter of the *ie*2 gene was replaced with a *lac*Z expression cassette driven by a human CMV *ie*1/*ie*2 gene promoter fragment used in previous recombinants (22), and (*ii*) a 600-bp *Bam*HI fragment including the putative polyadenylation signal for the γ0.85 transcript (3) was deleted. Progeny from transfection/infections were isolated by plaque purification using an overlay medium supplemented with 300 μg/ml of 5-bromo-4-chloro-3-indolyl-β-D-galactopyranoside (X-Gal) (CLONTECH) and 0.5% agarose. Further purification was performed by limiting dilution in 96-well culture dishes using culture medium supplemented with 150 μM 4-methylumbelliferyl β-D-galactoside (Sigma). Purity of recombinant virus was monitored by DNA blot hybridization after digestion with various restriction enzymes as well as by plaque assay and staining with X-Gal.

Experimental Infection of Mice. BALB/c mice at either 3–4 or 10 weeks of age (The Jackson Laboratory) were maintained (12) and inoculated by either the i.p. or s.c. (into footpads) route by using 1×10^6 to 5×10^6 plaque-forming units of virus. After CO_2 asphyxiation at indicated times, organs (22) and PB leukocytes (PBLs) (12) were harvested. Organs were sonicated and titered by plaque assay (22). Peritoneal exudate cells (PECs) were harvested at 48 h post-i.p. inoculation with 5×10^6 plaque-forming units of RM427$^+$ or from control mice by lavage with ice-cold PBS immediately after death. Washed PBLs, suspended in growth medium at 10^6 cells/ml, either were cytocentrifuged onto glass slides at 300 $\times$ *g* and were stained with X-Gal (300 μg/ml) in PBS (12, 23) or were subjected to an infectious center assay on NIH 3T3 cells overlaid with medium containing 0.75% carboxymethylcellulose. Batches of female mice were used for experiments approved by the Stanford University animal use and biosafety committees.

Calcium Mobilization. Free cytoplasmic calcium (Ca^{2+}) levels in PECs were measured by using a Zeiss Axiovert 135 microscope with Attofluor (Atto Instruments, Potomac, MD) attachments using Attofluor RATIOVISION and ATTOVISION software as described (24). Freshly prepared PECs were counted, were pelleted at 300 $\times$ *g* for 5 min at 4°C, were suspended at 2×10^6 cells/ml in growth medium, and were seeded at 8×10^5 cells/well into 8-chamber Lab-tek coverslip #1 chamber-wells (Nalge Nunc, Naperville, IL). After 2 h at 37°C in 5% CO_2, nonadherent cells were removed and saved for assay, and adherent cells were washed with PBS plus 1 mM $CaCl_2$ and 1 mM $MgCl_2$ (D-PBS). PBLs also were harvested as described above and were tested in this assay. All populations were incubated in 400 μl (per well) of D-PBS, 10% FCS, 10 mM glucose, and 1 μM Fura-2AM (Molecular Probes) (loading buffer) for 50 min at 37°C in 5% CO_2, were washed in D-PBS, 1% FCS, and 10 mM glucose (flux buffer), and were suspended in 400 μl flux buffer for assay. Fluorescence parameters used to detect Ca^{2+} flux were as described (24) with excitation by a split beam laser at 334 nm and 380 nm and emission collected at 520 nm. Samples were assayed at ambient (25°C) temperature. Fura-2AM-loaded nonadherent cells were allowed to settle to the bottom of the chamber wells for 45 min in 5% CO_2 after loading before being analyzed in the microscope. Cells were observed for 2–3 min under microscopic illumination before addition of chemokine, and spontaneous fluxing populations were discarded. Five to ten microliters of ionomycin (from a stock at 500 μg/ml in DMSO) (Sigma) was added to one chamber-well, and cell populations that were unresponsive to ionomycin were discarded. Chemokine in 5 μl of D-PBS, or control D-PBS, was added slowly (over a period of 3 sec) to reduce turbulence. Free Ca^{2+} levels were recorded from 20 sec before addition of chemokine until levels returned to background, typically a total period of 2 min. Recording was terminated after 1 min when no response was observed. Cells were defined as fluxing if the relative emission intensity ratio increased by 100% or more. All movies were made from sequential 2- to 3-sec interval frames by using Adobe Systems (Mountain View, CA) PREMIER software.

Free cytoplasmic Ca^{2+} levels were evaluated in populations of receptor-bearing cell lines by using a Photon Technology International (Princeton) spectrophotometer with excitation at 350 nm and dual emission recording at 400 nm and 490 nm after loading cells with INDO-1-AM (Molecular Probes) (20). Relative intracellular calcium levels were expressed as the 400 nm/490 nm emission ratio.

RESULTS

MCK-1 Activates PECs from Infected and Uninfected Mice. MCK-1 was chemically synthesized starting from a predicted signal peptide cleavage site (25) between amino acids 18 and 19 (Fig. 1*A*) and was tested for its ability to induce Ca^{2+} mobilization in adherent murine PECs and in single chemokine receptor-expressing cell lines. Intracellular Ca^{2+} mobilization was monitored in real time by digital fluorescence video microscopy (24) as well as by conventional spectrofluorometric methods (20). Intracellular Ca^{2+} levels in PECs from uninfected (Fig. 1 *B–D*) and virus-infected (Fig. 1 *E–G*) mice were compared 48 h after i.p. inoculation with a *lac*Z-tagged recombinant virus (RM427$^+$), a virus that was derived from murine CMV strain K181$^+$ (12) by insertion of a *lac*Z indicator gene disrupting the murine CMV *ie*2 gene. Importantly, this virus does not carry the *sgg*1 mutation found in a related virus, RM427 (22), or any mutations that would affect MCK-1 expression and exhibits the full growth potential of wild-type virus in cell culture and experimentally infected mice (ref. 26; data not shown). Prestimulation levels of free cytoplasmic Ca^{2+} remained low in all cells from uninfected as well as virus-infected mice (see Fig. 1B and 1E for examples). In both, MCK-1 induced a Ca^{2+} flux that peaked $\approx$12 sec after addition of MCK-1 to 250 nM (Fig. 1C and 1F) and returned to prestimulation levels within one (Fig. 1D) to two (Fig. 1G) min. The level of response to MCK-1 was consistently low in experiments using cells from uninfected and high using cells from virus-infected mice (Fig. 2*A* and 2B). Only 1.5–5.0% of adherent PECs from uninfected (Fig. 2A) whereas 30–60% from virus-infected mice (Fig. 2B) responded to MCK-1. Although these experiments did not assess whether the increase in MCK-1 responsive cells after infection was attributable to an innate host inflammatory response or virus-produced MCK-1, cells recruited to the peritoneal cavity were highly responsive to this chemokine homolog. Because synthetic chemokine was used for these experiments, polypeptide side chain modifications such as glycosylation that may occur in mammalian cells were shown to not be required for activity. Control manipulations such as the addition of D-PBS to PECs failed to induce flux (data not shown) and nonadherent PECs

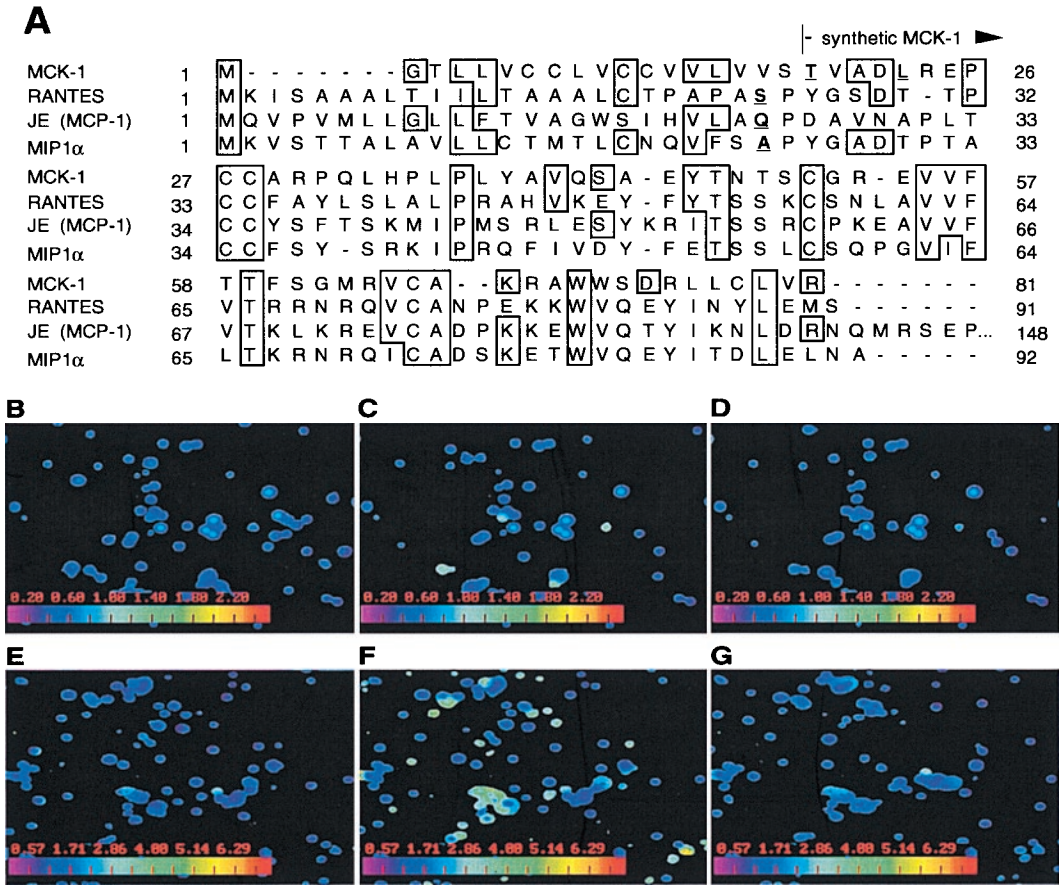

FIG. 1. MCK-1 induces Ca^{2+} signaling in murine PECs. (*A*). Predicted MCK-1 amino acid sequence (3) showing the similarity of this protein to three murine β chemokines, RANTES, JE (the homolog of human MCP-1), and MIP1α. The predicted signal sequence cleavage sites of the displayed chemokines are indicated in blue, including MCK-1 threonine 19, at which the synthetic MCK-1 peptide commences. (*B*–G). Digital fluorescence video microscopy frames of synthetic MCK-1 induced Ca^{2+} flux in glass-adherent PECs. Cells harvested by lavage from uninfected (*B–D*) or RM427$^+$-infected (*E–G*) 10-week-old BALB/c mice were labeled with 1 μM Fura-2-AM, and levels of free intracellular Ca^{2+} in individual cells, indicated on the digitally calculated color scale inserts on each panel, were measured by spectrofluorometric video microscopy before (*B* and *E*), 12 sec after addition of 250 nM MCK-1 (*C* and *F*), and 1 (*D*) and 2 (*G*) min later. The full series E-G can be viewed at http://cmgm.stanford.edu/~saederup/

as well as either adherent or nonadherent PBL populations from either virus- or mock-infected animals failed to respond to MCK-1 (<1–2% of cells responding; data not shown). These negative controls demonstrated that the synthetic MCK-1 preparation was not acting as a general mitogen or pyrogen. The specificity of MCK-1 for glass-adherent cells and the dramatic increase in responsiveness observed following infection strongly suggested that MCK-1 would be expected to influence the behavior of monocyte/macrophages attracted to sites of infection.

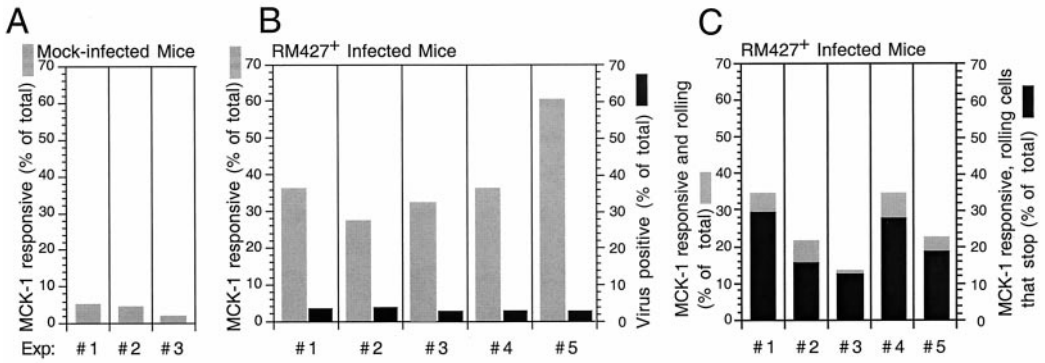

FIG. 2. MCK-1-induced Ca^{2+} flux leads to tight adherence. (*A*) Percentage of PECs from mock-infected mice responding to MCK-1, with three independent experiments shown. (*B*) Percentage of PECs from RM427$^+$-infected mice (48 h post-i.p. inoculation) responding to MCK-1 (gray bars), with results from five independent experiments shown. Percentage of PECs that were virus-infected based on β-galactosidase expression also is shown (black bars). The digital images shown in Fig. 1 of PECs from mock-infected mice are from experiment 2 (Exp. #2), and those from RM427$^+$-infected mice are from experiment 4. (*C*). Induction of tight adherence by MCK-1. The percentage of total adherent PECs that were loosely attached and that fluxed in response to MCK-1 (gray bars) and the percentage that adhered tightly to glass after responding to MCK-1 (black bars) are shown. Data are from the five experiments shown in *B*.

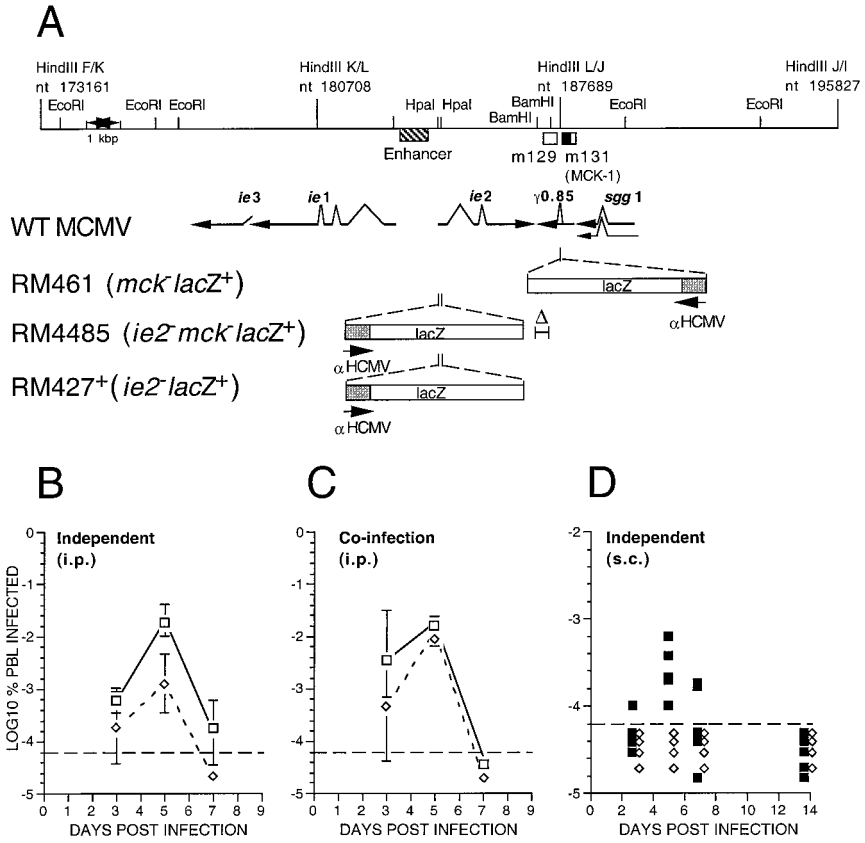

FIG. 3. Murine CMV MCK-1/MCK-2 mutant construction and evaluation of viremia during infection of mice. (*A*) Map of the *Hin*dIII K, L, and J fragments of wild-type murine CMV (WT MCMV; K181$^+$ strain) showing the position of the m129 and m131 ORFs (17), as open boxes, and the predicted MCK-1 ORF within m131 as a filled box. The murine CMV *ie*1/*ie*2/*ie*3 transcriptional enhancer and the arrangement of *ie*1, *ie*2, *ie*3, *sgg*1, and γ0.85 transcripts also are shown with splicing patterns indicated on the arrows depicting individual transcripts. The *lac*Z insertion mutations in the three recombinant viruses (RM461, RM4485, RM427$^+$) as well as the deletion mutation disrupting γ0.85 transcript expression in RM4485 are depicted below the map. The genome structure and growth properties of RM461, which carries a *lac*Z insert disrupting the γ0.85 transcript expression, has been described (12, 29). Expression of the *lac*Z gene in all recombinant viruses was regulated by a 199-bp human CMV *ie*1/*ie*2 promoter (αHCMV) fragment (−219 to −19 relative to the transcription start site) (22). This promoter fragment exhibits immediate early expression kinetics when adjacent to the murine CMV transcriptional enhancer, as in RM427$^+$ and RM4485, and delayed early expression kinetics in RM461 (12). (*B*) Levels of viremia after infection with K181$^+$ (□) or RM4485 (◇). BALB/c mice 3 or 4 weeks of age were inoculated by the i.p. route with 1×10^6 plaque-forming units of virus, and PBLs were harvested by heart puncture at 3, 5, and 7 days postinfection. Infection rates were expressed as the percentage of total PBLs that scored positive in an infectious centers assay on monolayers of NIH 3T3 cells. Error bars represent standard deviation of the means of titers in five mice. (*C*) Levels of viremia after co-infection with K181$^+$ and RM4485. Mice were co-inoculated by the i.p. route with a 1:1 mixture of K181$^+$ and RM4485 at 1×10^6 plaque-forming units, and PBLs were harvested as described in *B*. Infectious centers were stained to reveal β-galactosidase expression and to differentiate RM4485 from K181$^+$ plaques. (*D*) Levels of viremia after s.c. inoculation of RM427$^+$ (■) or RM4485 (◇) inoculated into one or two hind footpads were analyzed as above, except the results of individual mice were plotted as separate points. The dashed line in each panel represents the limit of detection.

To directly measure the proportion of PECs supporting productive viral infection, we stained cells from virus-infected mice with the β-galactosidase substrate X-Gal. This assay allows ready *in situ* discrimination between virus-infected and uninfected cells in tissues and has previously been used to investigate the distribution and dissemination of productively infected cells in infected mice (12). At 48 h postinoculation, ≈2–3% of adherent PECs from virus-infected mice were positive (Fig. 2*B*), indicating that only small a proportion of the MCK-1 responsive population could be productively infected. This data was consistent with previous reports that used conventional virus infectivity assays to show that only a small proportion of PECs actually become virus-positive at peak times of infection (27, 28).

Because video microscopy was carried out in real-time, we followed the adherence behavior of individual MCK-1 responsive cells from murine CMV-infected mice over the observation period. In these experiments, a significant proportion of cells were loosely adherent and drifted across the glass surface as a result of turbulence associated with injection of chemokine. As shown in Fig. 2*C*, nearly all loosely adherent cells stopped moving within seconds after fluxing and remained tightly anchored for the duration of the experiment. A Quicktime movie of signaling and adherence also can be viewed at http://cmgm.stanford.edu/~saederup/and is published as supplemental data on the PNAS web site, www.pnas.org.. The proportion of MCK-1-responsive cells from mock-infected mice was too low to assess their anchoring behavior. These data were consistent with the induction of adherence and suggested that leukocyte behavior may be altered by exposure to this viral gene product during the course of CMV infection.

The response of PECs to MCK-1 also implied that this activation may occur via particular chemokine receptors. When a variety of cell lines expressing individual human or mouse chemokine receptors were tested, only human CCR3, a natural receptor for eotaxin, RANTES, and MCP-3, was found to respond to MCK-1. Cross-ligand desensitization on CCR3 cells showed that MCK-1-induced signaling via human CCR3 was specific, as prior exposure to human eotaxin completely abrogated any human CCR3-specific MCK-1 response. The human macrophage cell line THP1 also responded to MCK-1 (data not shown). Cells bearing other chemokine receptors,

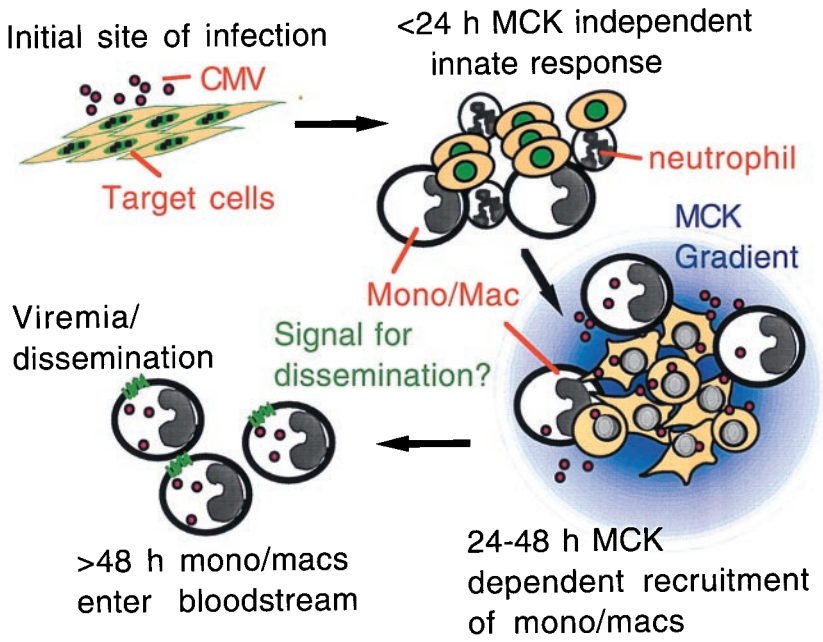

FIG. 4. Impact of MCK-1/MCK-2 on viral infection. After inoculation of murine CMV, virus gene expression and DNA replication ensues within the first 24 h and is accompanied by an innate inflammatory response. As virus-infected cells begin producing progeny virus, the MCK-1/MCK-2 gene product is made and either sustains or increases the recruitment of a permissive monocyte/macrophage (Mono/Mac) population that can be directed efficiently to blood by an as yet unknown (but possibly MCK-1/MCK-2-determined) process that results in more efficient dissemination.

including human CCR1, CCR2B, and CCR5, murine CCR3, or human CMV US28, were unresponsive to MCK-1. In addition to not responding, these cells were not antagonized by MCK-1 as measured by sequential addition of MCK-1 and a relevant positive control chemokine (RANTES on CCR1 or US28, MCP-3 on CCR2B, RANTES or MIP1α on CCR5, and eotaxin on murine CCR3) (data not shown). These results directly demonstrate that MCK-1 can specifically induce a signal via a chemokine receptor, human CCR3. Together with our observations of agonist activity on PECs, this suggests a role for MCK-1 as a chemokine recruiting and/or activating monocytes or macrophages during infection. It seems unlikely that MCK-1 uses murine CCR3 as its natural receptor during infection, given the lack of any detectable agonist or antagonist activity on a cell line bearing this receptor. MCK-1 may engage some other murine chemokine receptor with structural properties related to human CCR3.

Disruption of MCK-1/MCK-2 Correlates with Decreased Viremia and Dissemination. Previous efforts to understand dissemination of murine CMV via PBLs used RM461, a *lac*Z-tagged recombinant virus with an insertion mutation in the γ0.85 transcript (3) that is now known to encode MCK-1 and/or MCK-2 (7, 12). Although RM461 exhibited wild-type levels of growth in cultured fibroblasts as well as in spleen, liver, lungs, and adrenals of mice after i.p. inoculation (29), and also retained full virulence and latency characteristics (12), this virus exhibited consistently low growth levels in salivary glands (12, 29) when studied in BALB/c mice. This phenotype was maintained in T cell deficient nude and severe combined immunodeficient mice. Because of our finding here that MCK-1 exhibited chemokine-like activity, we examined the behavior of viruses carrying mutations affecting MCK-1/MCK-2 expression with specific attention to alteration of the secondary viremia that precedes dissemination to salivary glands (12, 14). We constructed a mutant virus, RM4485, carrying a deletion mutation disrupting the γ0.85 transcript (Fig. 3*A*). Both RM4485 and the control virus RM427$^+$ carry a *lac*Z insertion disrupting the *ie*2 gene, previously shown to be dispensable for infection, dissemination, and latency in mice (26, 29, 30). The deletion mutation in RM4485 eliminated the γ0.85 transcript based on RNA blot as well as reverse transcription PCR analyses (data not shown). Consistent with previous studies using RM461 (12, 29, 30), both RM427$^+$ and RM4485 exhibited replication properties in cultured fibroblasts and in the spleen, liver, and lungs of experimentally inoculated (i.p.) mice that were similar to those achieved by parental virus, indicating that the primary viremia that seeds these organs was not affected by the MCK-1/MCK-2 mutation (data not shown). The secondary viremia induced by mutant virus was reduced 20- to 50-fold compared with either parental K181$^+$ (Fig. 3*B*) or *lac*Z-tagged control RM427$^+$ virus (data not shown). RM4485 peak viremia was similar to that previously reported for RM461 (12) in work that implicated large mononuclear, glass-adherent phagocytes as cells that disseminate infection. Furthermore, as expected from previous work with RM461 (12, 29), the disruption of the γ0.85 transcript in RM4485 reduced peak levels of virus replication in salivary glands by 2–3 orders of magnitude relative to control viruses (data not shown), consistent with the role of secondary viremia in seeding this organ (14). Co-infection with RM4485 and K181$^+$, whose plaques were distinguished by staining with X-Gal, resulted in complementation of the RM4485 defect and the detection of wild-type levels of viremia for both viruses (Fig. 3*C*) in a pattern that was consistent with an impact by a trans-acting viral factor on monocyte/macrophage trafficking. When subcutaneous inoculation in footpads was carried out, both mutant and wild-type virus replicated equally well at the site of inoculation (data not shown), but viremia was detected only in animals inoculated with virus carrying an intact MCK-1/MCK-2 gene (Fig. 3*D*). Thus, the MCK-1/MCK-2 are important determinants of the secondary viremia that mediates dissemination to the salivary glands.

DISCUSSION

Murine CMV replicates broadly in the host during acute infection as a result of dissemination from the initial sites of infection, with organs such as spleen, liver, lungs, and, particularly, salivary glands involved (31). Active replication is initially controlled via innate immune mechanisms, primarily

natural killer cells, but also neutrophils and monocyte/macrophages (32–35). Subsequently, the virus is cleared by an adaptive T-lymphocyte-mediated response (36, 37). Interestingly, leukocytes are also vehicles for dissemination of murine CMV from initial sites of infection, which suggests that their behavior may be controlled by virus. This report and work on human CMV (6) indicates that viral chemokine homologs may play integral roles recruiting leukocytes subclasses that are required for efficient dissemination.

We show that murine CMV MCK-1 can signal via a chemokine receptor and has chemokine-like activities on peritoneal macrophages, which is enhanced by viral infection. Along with our observation of reduced viremia when virus fails to express MCK-1/MCK-2, our results highlight the role of a viral gene mimetic of host chemokines as a determinant of spread during acute infection within the natural host. Our results suggest a model in which chemokine homologs may promote survival and dissemination to organs such as salivary glands in ways that mimic host functions that control leukocyte trafficking during the immune response. This model is depicted in Fig. 4. Innate immune responses result in the recruitment of leukocytes to sites of murine CMV infection, where the eventual expression of MCK-1/MCK-2 (>24 h postinfection) may ensure the attraction of a particular mononuclear phagocyte suited to optimal viral spread. MCK-1/MCK-2 may also alter permissiveness and/or trafficking behavior, allowing infected monocyte/macrophages to leave the site of inflammation and enter the bloodstream. MCK-1/MCK-2 appears to be critical for maximal levels of secondary viremia, which occurs at 5–6 days postinoculation, in a pattern that reflects the regulatory class of this gene as a $\gamma 2$ (true late) function (3). The dependence on MCK-1/MCK-2 suggests that secondary viremia perhaps requires an active manipulation of host cells to achieve maximal dissemination. We predict that this function is likely to be critical to successful infection at the low infectious doses encountered during natural infection. Consistent with this prediction, MCK-1/MCK-2 mutants do not sustain as intense an inflammation as wild-type virus in footpads, consistent with a role in maintaining monocyte migration to sites of infection (Shirley Aguirre, N.S., and E.S.M., unpublished observations). Although our data do not rule out some as yet undetected MCK-1/MCK-2 role in blocking efficient viral clearance (33–35), our previous finding that MCK-1/MCK-2 mutant virus exhibits the same levels of reduced dissemination in immunocompetent BALB/c, as well as immunodeficient BALB/nude and C.B17 SCID mice (12), argues strongly that MCK-1/MCK-2 is acting independent of an adaptive, T lymphocyte immune response.

Murine CMV is to date the only virus that expresses a chemokine homolog whose role has been studied in the natural host. *In vitro* studies on other viral chemokines are, however, starting to produce intriguingly analogous results. Human CMV, which associates with neutrophils and may disseminate via this leukocyte subset in immunocompromised individuals (38, 39), encodes an α chemokine (UL146) that functions as a potent neutrophil chemoattractant (6). Kaposi's sarcoma-associated herpesvirus-encoded vMIP-II, which has been ascribed a role in skewing the immune response (10), may act as an agonist to attract cells that aid this virus in dissemination. Our evidence that murine CMV MCK-1/MCK-2 dramatically influences levels of viremia provides a clear example of the uses to which pirated host functions can be put after incorporation into a viral genome.

We acknowledge Shirley Aguirre for help with mouse inoculation and for helpful discussion and thank Dan Littman for providing chemokine receptor-bearing cell lines. This work was supported by grants from the U.S. Public Heath Service (Grants RO1 AI28341 and RO1 AI30363). N.S. was supported by U.S. Public Heath Service Training Grant T32 GM07328.

1. Dairaghi, D. J., Greaves, D. R. & Schall, T. J. (1998) *Semin. Virol.* **8,** 377–385.
2. Baggiolini, M., Dewald, B. & Moser, B. (1997) *Annu. Rev. Immunol.* **15,** 675–705.
3. MacDonald, M. R., Li, X. Y. & Virgin, H. W., IV (1997) *J. Virol.* **71,** 1671–1678.
4. Kledal, T. N., Rosenkilde, M. M., Coulin, F., Simmons, G., Johnsen, A. H., Alouani, S., Power, C. A., Luttichau, H. R., Gerstoft, J., Clapham, P. R., *et al.* (1997) *Science* **277,** 1656–1659.
5. Boshoff, C., Endo, Y., Collins, P. D., Takeuchi, Y., Reeves, J. D., Schweickart, V. L., Siani, M. A., Sasaki, T., Williams, T. J., Gray, P. W., *et al.* (1997) *Science* **278,** 290–294.
6. Penfold, M. E. T., Dairaghi, D. J., Duke, G. M., Saederup, N., Mocarski, E. S., Kemble, G. W. & Schall, T. J. (1999) *Proc. Natl. Acad. Sci. USA*, in press.
7. MacDonald, M. R., Burney, M. W., Resnick, S. B. & Virgin, H. W., IV (1999) *J. Virol.* **73,** 3682–3691.
8. Damon, I., Murphy, P. M. & Moss, B. (1998) *Proc. Natl. Acad. Sci. USA* **95,** 6403–6407.
9. Krathwohl, M. D., Hromas, R., Brown, D. R., Broxmeyer, H. E. & Fife, K. H. (1997) *Proc. Natl. Acad. Sci. USA* **94,** 9875–9880.
10. Sozzani, S., Luini, W., Bianchi, G., Allavena, P., Wells, T. N., Napolitano, M., Bernardini, G., Vecchi, A., D'Ambrosio, D., Mazzeo, D., *et al.* (1998) *Blood* **92,** 4036–4039.
11. Revello, M. G., Zavattoni, M., Sarasini, A., Percivalle, E., Simoncini, L. & Gerna, G. (1998) *J. Infect. Dis.* **177,** 1170–1175.
12. Stoddart, C. A., Cardin, R. D., Boname, J. M., Manning, W. C., Abenes, G. B. & Mocarski, E. S. (1994) *J. Virol.* **68,** 6243–6253.
13. Bale, J. F., Jr & O'Neil, M. E. (1989) *J. Virol.* **63,** 2667–2673.
14. Collins, T. M., Quirk, M. R. & Jordan, M. C. (1994) *J. Virol.* **68,** 6305–6311.
15. Mocarski, E. S. (1996) in *Fields Virology*, eds. Fields, B. N., Knipe, D. M. & Howley, P. M. (Lippincott–Raven, New York), pp. 2447–2492.
16. Ho, M. (1991) *Cytomegalovirus: Biology and Infection* (Plenum, New York).
17. Rawlinson, W. D., Farrell, H. E. & Barrell, B. G. (1996) *J. Virol.* **70,** 8833–8849.
18. Vieira, J., Farrell, H. E., Rawlinson, W. D. & Mocarski, E. S. (1994) *J. Virol.* **68,** 4837–4846.
19. Deng, H., Liu, R., Ellmeier, W., Choe, S., Unutmaz, D., Burkhart, M., Di Marzio, P., Marmon, S., Sutton, R. E., Hill, C. M., *et al.* (1996) *Nature (London)* **381,** 661–666.
20. Dairaghi, D. J., Oldham, E. R., Bacon, K. B. & Schall, T. J. (1997) *J. Biol. Chem.* **272,** 28206–28209.
21. Neote, K., DiGregorio, D., Mak, J. Y., Horuk, R. & Schall, T. J. (1993) *Cell* **72,** 415–425.
22. Manning, W. C., Stoddart, C. A., Lagenaur, L. A., Abenes, G. B. & Mocarski, E. S. (1992) *J. Virol.* **66,** 3794–3802.
23. Ho, D. Y. & Mocarski, E. S. (1988) *Virology* **167,** 279–283.
24. Wulfing, C., Sjaastad, M. D. & Davis, M. M. (1998) *Proc. Natl. Acad. Sci. USA* **95,** 6302–6637.
25. Nielsen, H., Engelbrecht, J., Brunak, S. & von Heijne, G. (1997) *Int. J. Neural Syst.* **8,** 581–599.
26. Lin, Y.-C. (1997) Ph.D. thesis (Stanford Univ., Stanford, CA), pp. 213.
27. Mims, C. A. & Gould, J. (1978) *J. Gen. Virol.* **41,** 143–153.
28. Brautigam, A. R., Dutko, F. J., Olding, L. B. & Oldstone, M. B. (1979) *J. Gen. Virol.* **44,** 349–359.
29. Cardin, R. D., Boname, J. M., Abenes, G. B., Jennings, S. A. & Mocarski, E. S. (1993) in *Multidisciplinary Approaches to Understanding Cytomegalovirus Disease*, eds. Plotkin, S. & Michelson, S. (Elsevier, Amsterdam), pp. 101–110.
30. Cardin, R. D., Abenes, G. B., Stoddart, C. A. & Mocarski, E. S. (1995) *Virology* **209,** 236–241.
31. Mocarski, E. S., Abenes, G. B., Manning, W. C., Sambucetti, L. C. & Cherrington, J. M. (1990) *Curr. Top. Microbiol. Immunol.* **154,** 47–74.
32. Shellam, G. R., Allan, J. E., Papadimitriou, J. M. & Bancroft, G. J. (1981) *Proc. Natl. Acad. Sci. USA* **78,** 5104–5108.
33. Welsh, R. M., Brubaker, J. O., Vargas-Cortes, M. & O'Donnell, C. L. (1991) *J. Exp. Med.* **173,** 1053–1063.
34. Scalzo, A. A., Fitzgerald, N. A., Wallace, C. R., Gibbons, A. E., Smart, Y. C., Burton, R. C. & Shellam, G. R. (1992) *J. Immunol.* **149,** 581–589.
35. Lathbury, L. J., Allan, J. E., Shellam, G. R. & Scalzo, A. A. (1996) *J. Gen. Virol.* **77,** 2605–2613.
36. Koszinowski, U. H., del Val, M. & Reddehase, M. J. (1990) *Curr. Top. Microbiol. Immunol.* **154,** 189–220.
37. Lucin, P., Pavic, I., Polic, B., Jonjic, S. & Koszinowski, U. H. (1992) *J. Virol.* **66,** 1977–1984.
38. Grundy, J. E., Lawson, K. M., MacCormac, L. P., Fletcher, J. M. & Yong, K. L. (1998) *J. Infect. Dis.* **177,** 1465–1474.
39. Revello, M. G., Percivalle, E., Arbustini, E., Pardi, R., Sozzani, S. & Gerna, G. (1998) *J. Clin. Invest.* **101,** 2686–2692.